Rapid Communications

Unveiling two deuteration effects on hydrogen-bond breaking process of water isotopomers

Fumiaki Kato,[1] Toshiki Sugimoto,[2,3,*] Kuniaki Harada,[1] Kazuya Watanabe,[1] and Yoshiyasu Matsumoto[4]

[1]*Department of Chemistry, Graduate School of Science, Kyoto University, Kyoto 606-8502, Japan*

[2]*Department of Materials Molecular Science, Institute for Molecular Science, Myodaiji, Okazaki, Aichi 444-8585, Japan*

[3]*Precursory Research for Embryonic Science and Technology (PRESTO), Japan Science and Technology Agency (JST), Saitama 332-0012, Japan*

[4]*Toyota Physical and Chemical Research Institute, 41-1 Yokomichi, Nagakute, Aichi 480-1192, Japan*

(Received 26 September 2018; revised manuscript received 25 July 2019; published 27 November 2019)

The quantum nature of hydrogen bonds in water manifests itself in peculiar physicochemical isotope effects: While deuteration often elongates and weakens the hydrogen bonds of typical hydrogen-bonded systems composed of bulky constituent molecules, it elongates but strengthens the hydrogen bonds of water molecular aggregates. The origin of this unique isotope effect of water molecules remains to be elucidated at the molecular level. By means of isotope-selective measurements on the sublimation of water ices with various H/D compositions, we disentangle two opposite deuteration effects on the hydrogen-bond breaking process of water molecules: (1) Deuterating a desorbing water molecule increases the energy needed for desorption E_d, while (2) deuterating water molecules neighboring a desorbing molecule reduces its E_d. The increase in E_d originates from zero-point energy in the hindered rotation of the desorbing molecule, whereas the decrease in E_d is caused by quantum anharmonic couplings between the inter- and intramolecular vibrational modes involved in the hydrogen-bonding interactions of desorbing water molecules. On the basis of these findings, we discuss the peculiar nature of hydrogen bonds of water molecules in comparison with bulky hydrogen-bonded molecules.

DOI: 10.1103/PhysRevMaterials.3.112001

The physicochemical and biological properties of hydrogen-bonded systems are significantly affected by nuclear quantum effects (NQEs) including the zero-point energies of vibrational modes and proton tunneling and delocalization [1–5]. These originate from the extremely low nuclear mass of hydrogen; thus, hydrogen-bonded systems show remarkable isotope effects upon deuteration. For typical hydrogen-bonded molecules such as oxalic acid dihydrate, benzoic acid, and succinic acid, deuterium substitution elongates their hydrogen bonds; this geometrical isotope effect has been known as the Ubbelohde isotope effect since the 1930s [6–12]. In such hydrogen-bonded systems composed of bulky constituent molecules, deuteration also decreases the melting-point temperatures and energies needed for breaking hydrogen bonds [13,14], in line with the robust relationship: Longer bonds have a smaller binding energy [15,16]. These results are thus considered as pieces of evidence for the weakening of hydrogen bonds by deuterium substitution [6–14]. In comparison with those hydrogen-bonded systems, water molecular aggregates such as liquid water and ice exhibit unique isotope effects on their thermodynamic properties [17–27]: Although deuterium substitution increases the intermolecular distance between water molecules [22,23], it also *increases* the melting and boiling points, and vaporization enthalpy [24–27]. This leads to an interesting question on the binding energy of water aggregates: Why do *more expanded* D_2O aggregates form *stronger* hydrogen bonds than H_2O aggregates, in contrast to the hydrogen-bonded systems composed of bulky constituent molecules? The molecular-level origin of this question has not been elucidated in a unified way.

In the last decade, intensive studies have been conducted to elucidate NQEs on water hydrogen bonds [5,27–33]. Most of these studies have focused on the structural and dynamical properties of an O-H $\cdots$ O type hydrogen bond in condensed (bonded) states [5,27–33]; thus, NQEs relevant to the isotopic differences of the binding energy of water molecules have not been explicitly considered. In addition, previous experimental studies have focused only on a simple comparison among isotopically pure water samples: H_2O vs D_2O [24,25]. In the present Rapid Communication, we shed light on the isotope effect on the desorption of water molecules from the surfaces of crystalline and amorphous ices with various H/D isotopic compositions (the deuterium mole fraction x_D). Because water molecules have no activation barrier for adsorption to ice surfaces [34], the activation energy for desorption E_d derived from temperature programmed desorption (TPD) directly corresponds to the binding energy of water molecules. Moreover, the isotope-selective detection of the desorption rates of H_2O, HDO, and D_2O molecules enables us to obtain E_d for three water isotopomers as a function of x_D. With these techniques, we succeeded in experimentally demonstrating that two types of deuteration effects competitively determine the isotope effects on the binding energy of water molecules, which allows us to discuss the peculiar isotope effect of water aggregates in comparison with hydrogen-bonded systems composed of bulky constituent molecules.

*Corresponding author: toshiki-sugimoto@ims.ac.jp

The experiments were conducted in an ultrahigh vacuum chamber with a base operating pressure below 5×10^{-8} Pa [35–37]. Isotope-mixed crystalline ice with a thickness of 10–250 bilayers (BL, 1 BL $\sim 1.1 \times 10^{19}$ m^{-2}) were grown on Pt(111) at 140 K by backfilled vapor deposition of pre-isotope-mixed water. Hexagonal crystalline-ice films with wide terraces of a basal plane have been reported to grow on Pt(111) in a layer-by-layer growth mode when the ice samples are sufficiently thick ($\gtrsim$50 BL) [38–42]. The isotope composition of premixed water vapor was measured with a calibrated quadrupole mass spectrometer (QMS) during backfilled vapor deposition. The isotope compositions of all isotope-mixed water vapors were in the equilibrium condition of the H/D exchange reaction ($H_2O + D_2O \rightleftharpoons 2HDO$) [43,44] [Fig. S1(a)] at $K_{H/D} = [HDO]^2/[H_2O][D_2O] \sim 4$ [44–46] (see also Supplemental Material Sec. 9 [47]). Thus, the deuterium mole fraction x_D is the only parameter for determining the isotope composition of ice samples (Fig. S1). After preparation of an ice film, the TPD measurement was performed at a heating rate of 0.1 K/s.

First, we examined the initial thickness dependence of TPD traces to elucidate the kinetic order of the desorption reaction. The desorption rates of all water isotopomers were independent of ice film thickness [Figs. 1(a)–1(c)], exhibiting a feature characteristic of zero-order desorption from a surface with a constant area [24,25,42,48]. Thus, the rate of each water isotopomer is given by

$$\frac{d\theta_X(T)}{dt} = [X]k_d^X(T) = [X]v_0^X \exp\left[-\frac{E_d^X}{k_B T}\right], \qquad (1)$$

where θ_X is the total adsorbed amount of water isotopomers X ($X = H_2O$, HDO, and D_2O), $[X]$ is the surface mole fraction of X, and k_d^X is the Arrhenius-type rate constant expressed by the preexponential factor v_0^X, the activation energy for desorption E_d^X, the Boltzmann constant k_B, and the absolute temperature T. Therefore, Figs. 1(a)–1(c) indicate that k_d^X is independent of film thickness and $[X]$ remains almost constant during sublimation. Figure 1(d) shows the temperature dependence of the isotope composition in the isotope-mixed ice films estimated from TPD traces, indicating that isotope fractionation (deuterium enrichment) in the ice films is negligibly small (less than ~1%) in our experiments.

As shown in Fig. 2(a), $k_d^X(T)$ of each isotopomer decreases with increasing x_D. E_d^X and v_0^X were derived from the Arrhenius plots of $k_d^X(T)$ [Fig. 2(b)] as a function of x_D as shown in Figs. 2(c) and S3, respectively. Note that the values of these parameters did not depend on the temperature range used for the fitting analysis, indicating that there is no false compensation effect [49] in the analysis. E_d and v_0 for the sublimation of pure-H_2O ($x_D = 0$) ice were estimated to be 55.1 ± 1.3 kJ/mol and $4.0 \times 10^{17\pm0.3}$ BL/s, respectively, while those of almost pure-D_2O ice ($x_D \sim 1.0$) were 57.6 ± 1.7 kJ/mol and $9.2 \times 10^{17\pm0.4}$ BL/s, respectively. These values are in good agreement with those reported previously [24,25]. Therefore, E_d for D_2O desorption from pure-D_2O ice is slightly larger than that for H_2O desorption from pure-H_2O ice.

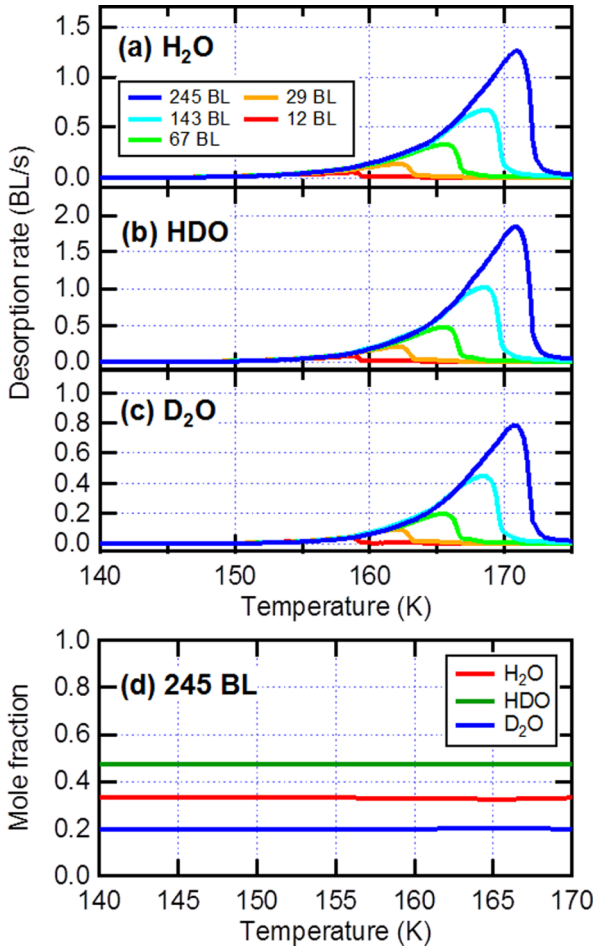

FIG. 1. Temperature dependence of desorption rates of (a) H_2O, (b) HDO, and (c) D_2O from the isotope-mixed crystalline ice ($x_D = 0.44$) with various initial film thicknesses. (d) Temperature dependence of isotope compositions of remaining ice estimated from the TPD traces of ice film with an initial thickness of 245 BL at $x_D = 0.44$.

Two types of interesting isotope effects on the strength of hydrogen bonds are clearly exhibited in Fig. 2(c): (1) $E_d^{H_2O} < E_d^{HDO} < E_d^{D_2O}$ is satisfied at any x_D, indicating that hydrogen bonds are strengthened when hydrogen of a desorbing molecule is substituted by deuterium; and (2) E_d^X decreases with increasing x_D for all isotopomers, indicating that they are weakened when the hydrogen of water molecules surrounding the desorbing molecule is substituted by deuterium. These opposite deuteration effects compete with each other on the binding energy of the water isotopomers. Although the small difference in E_d between pure-H_2O ice [$E_d^{H_2O}$ ($x_D = 0$)] and pure-D_2O ice [$E_d^{D_2O}$ ($x_D = 1$)] has been mostly attributed to effect (1) derived from the isotopic difference of a desorbing molecule [24,25], our results clearly indicate that the isotope effect on the strength of hydrogen bonds in water ice is determined by a delicate balance between the two competing deuteration effects (1) and (2).

To confirm whether the competitive deuteration effects emerge in the desorption from other forms of water aggregates, we also conducted the same TPD measurements for

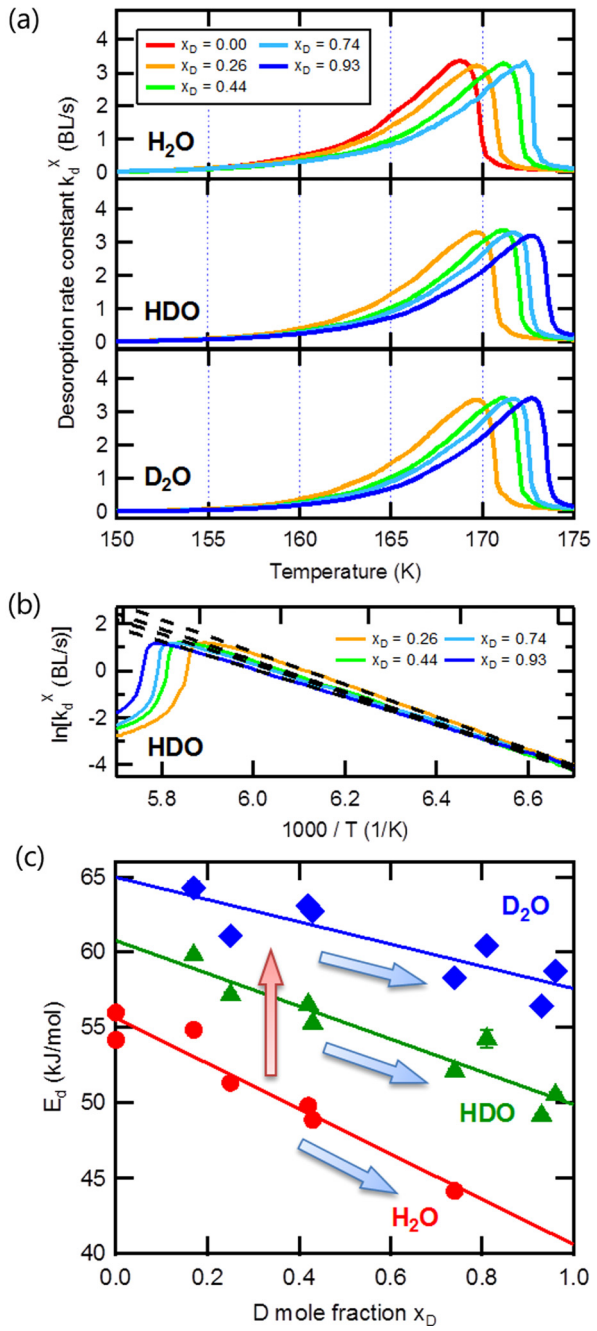

FIG. 2. TPD traces of isotope-mixed crystalline ice with various x_D. (a) x_D dependence of $k_d^X(T) \equiv -\frac{1}{[X]}\frac{d\theta_X(T)}{dt}$ of each isotopomer for ice films with 240-BL thickness. (b) Typical example of Arrhenius plots of $k_d^X(T)$ (color lines) and results of linear fitting (dashed black lines). (c) Activation energy for desorption of each isotopomer as a function of x_D.

isotope-mixed amorphous ice (Supplemental Material Sec. 6 [47]). As clearly shown in Fig. S6, the same deuteration effects (1) and (2) were observed. Moreover, as described in the Supplemental Material Sec. 7 [47], we found that even the evaporation behavior of liquid water shows a similar isotope dependence (Fig. S7). These results suggest that water aggregates have in common these competing deuteration effects (1) and (2) in the complete breaking process of hydrogen bonds during desorption.

The important features of these competing deuteration effects can be reasonably understood in a framework of the transition state theory (TST) [24,50]. In this framework, as schematically shown in Fig. 3(a), E_d is given as

$$E_d = E_0 + \sum_i \left(\mathrm{ZPE}_i^{\mathrm{TS}} - \mathrm{ZPE}_i^{\mathrm{IS}}\right), \tag{2}$$

where E_0 is the height of the potential-energy barrier for desorption measured from the potential-energy minimum, and $\mathrm{ZPE}_i^{\mathrm{TS}}$ and $\mathrm{ZPE}_i^{\mathrm{IS}}$ are the zero-point energies of the ith vibrational mode of a desorbing molecule at the transition state (TS) and the initial state (IS), respectively (see also Supplemental Material Secs. 2 and 3 [47]). IS is defined as the adsorbed state of a water molecule on an ice surface [51–53], where all inter- and intramolecular motions of the molecule are characterized with three intramolecular vibrations, three hindered rotations, and three hindered translations. Because there are no activation barriers for the adsorption of water molecules on the ice surface [34], we can define TS as a state in the gas phase [24], where a molecule has three intramolecular vibrations, three free rotations, and three free translations.

The first isotope effect on E_d, i.e., $E_d^{\mathrm{H_2O}} < E_d^{\mathrm{HDO}} < E_d^{\mathrm{D_2O}}$, is attributed to the difference in the zero-point energy of a desorbing molecule: $\sum_i(\mathrm{ZPE}_i^{\mathrm{TS}} - \mathrm{ZPE}_i^{\mathrm{IS}})$ [24]. Although the zero-point energies of the intramolecular vibrational modes are large (Table S1), these modes contribute little to E_d because of the relatively small zero-point-energy differences between TS and IS (Table S2). In contrast, intermolecular vibrational modes such as hindered translational and rotational modes in IS can largely contribute to E_d because the zero-point energies of free translations and rotations at TS are zero ($\mathrm{ZPE}_i^{\mathrm{TS}} = 0$). Note that the principal moments of inertia of a water molecule are much more sensitive to deuterium substitution than its total mass (Table S3) [24]. Moreover, the typical vibrational frequency of hindered rotation ($\sim$800 cm^{-1}) is much higher than that of hindered translation ($\sim$200 cm^{-1}) [54]. Thus, the hindered rotations of a desorbing molecule dominantly contribute to the first isotope effect on E_d (see also Supplemental Material Sec. 8 [47]); deuterated water species effectively strengthen hydrogen bonds ($E_d^{\mathrm{H_2O}} < E_d^{\mathrm{HDO}} < E_d^{\mathrm{D_2O}}$) due to the markedly reduced zero-point energies of the hindered rotation upon deuterium substitution [Fig. 3(b) and Table S2]. Our interpretation also describes well the previous experimental results that the desorption energy of $H_2{}^{18}O$ is almost the same as that of $H_2{}^{16}O$ but smaller than that of D_2O for both ice and liquid water [24,26].

The origin of the second isotope effect, i.e., x_D dependence of E_d, would be different from that of the desorbing isotopomer dependence discussed above; as shown in Fig. 3(c), the x_D dependence of E_d can be ascribed to the dependence of the potential-well depth E_0 on x_D (see also Supplemental Material Sec. 4). As discussed in the following, E_0 becomes smaller for deuterium-rich ice than hydrogen-rich ice because of the anharmonic coupling between intermolecular vibrational modes (hindered translational motions) and intramolecular O-H(O-D) stretching modes of water molecules donating a hydrogen bond to the desorbing molecule. Here, we demonstrate the essential feature of this isotope effect by using a one-dimensional model of the O-H(D)$\cdots$O type

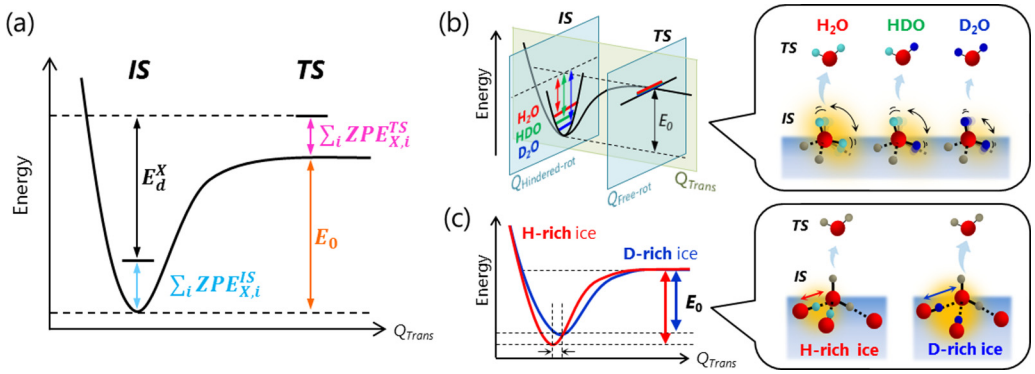

FIG. 3. (a) Schematic energy diagram for desorption. (b) The origin of isotope dependence of activation energy for desorption derived from the isotopic difference in the zero-point energy of hindered rotational modes of a desorbing molecule at the initial state (IS). (c) The origin of x_D dependence of activation energy derived from the isotopic difference in the potential energy surface for desorption. Red, white, and blue spheres are O, H, and D atoms, respectively. The gray sphere indicates H or D atoms.

hydrogen bond [Fig. 4(a)]. The total Hamiltonian of the model system is given as

$$\hat{H}(r_{\mathrm{OH(D)}}, R_{\mathrm{OO}}) = \hat{K}_{\mathrm{OH(D)}}(r_{\mathrm{OH(D)}}) + \hat{K}_{\mathrm{OO}}(R_{\mathrm{OO}}) + V(r_{\mathrm{OH(D)}}, R_{\mathrm{OO}}), \quad (3)$$

where $\hat{K}_{\mathrm{OH(D)}}$ and $\hat{K}_{\mathrm{OO}}$ are the kinetic energy terms of O-H(O-D) stretching and O-O intermolecular modes, respectively, and $V(r_{\mathrm{OH(D)}}, R_{\mathrm{OO}})$ is the potential energy term as a function of O-H(O-D) bond length $r_{\mathrm{OH(D)}}$ and the O-O distance R_{OO}. We adopted the potential energy of the Lippincott-Schroeder (LS) model [Fig. 4(b)] [55–58] with the parameters used for hexagonal crystalline ice (ice-Ih) [56,57]. In this model, the following key feature of water hydrogen bonds is explicitly included: The potential energy curve along $r_{\mathrm{OH(D)}}$ becomes more anharmonic as R_{OO} decreases [Fig. 4(c)]. Because the frequencies of O-H(O-D) stretching modes are about one order of magnitude higher than that of the intermolecular O-O vibration, we can reasonably solve the Schrödinger equation with respect to $r_{\mathrm{OH(D)}}$ and R_{OO} under the adiabatic approximation [59] (see Supplemental Material Sec. 5 [47] for details). In this approximation, the adiabatic intermolecular potential $V_{\mathrm{ad}}(R_{\mathrm{OO}})$ for the O-H(D)$\cdots$O hydrogen bond [Fig. 4(d)] is obtained by deriving the eigenenergy of a vibrational ground state of O-H(O-D) stretching modes for a fixed R_{OO} [Fig. 4(c)] and then plotting them as a function of R_{OO}.

The zero-point-energy difference in the anharmonic potential energy curve between O-H and O-D stretching modes [Fig. 4(c)] causes an isotopic difference in the adiabatic potential $V_{\mathrm{ad}}(R_{\mathrm{OO}})$ [Fig. 4(d)]. The depth of $V_{\mathrm{ad}}(R_{\mathrm{OO}})$ corresponding to E_0 of a hydrogen bond for the O-D$\cdots$O system is smaller than that for the O-H$\cdots$O system. In addition, the equilibrium intermolecular O-O distance of the O-D$\cdots$O bond becomes longer than that of the O-H$\cdots$O bond. The estimated isotopic difference in the O-O distance is about 0.3%, in good agreement with experimental observation [22] and quantum calculations [23] of the geometric isotope effect in ice. Thus, this model describes well the essential feature of the Ubbelohde effect; deuterium substitution of hydrogen donating a water molecule makes the hydrogen bond longer and weaker in terms of the binding energy [Figs. 3(c) and 4(d)]. Because this important feature emerges as a result of the quantum anharmonic couplings between inter- and

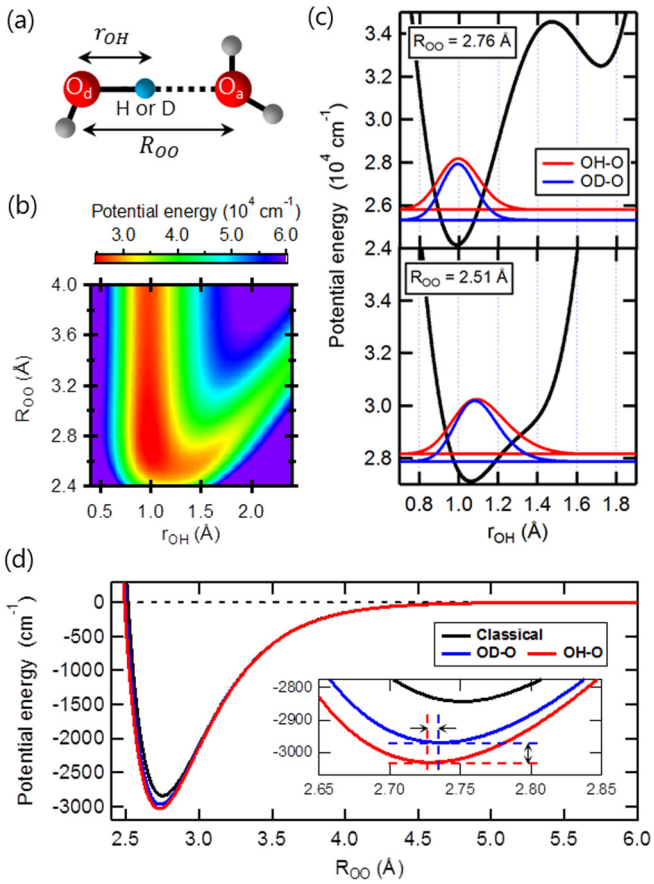

FIG. 4. (a) The definition of two variables $r_{\mathrm{OH(D)}}$ and R_{OO} used in the dimer model. (b) Two-dimensional plot of the Lippincott-Schroeder potential energy surface $V_{\mathrm{LS}}(r_{\mathrm{OH(D)}}, R_{\mathrm{OO}})$. Parameters were shown in Table S4 (Supplemental Material Sec. 5 [47]). (c) The eigenenergies (colored straight lines) and the eigenfunctions (colored curved lines) for the vibrational ground states of O-H and O-D stretching modes in the potential $V(r_{\mathrm{OH(D)}}, R_{\mathrm{OO}})$ (black lines) at typical $R_{\mathrm{OO}} = 2.76$ (upper panel) and 2.51 Å (lower panel). (d) Adiabatic intermolecular potential for O-H$\cdots$O and O-D$\cdots$O hydrogen bonds. Inset: Enlarged view around the potential minimum.

intramolecular vibrational modes included in the LS model [Eq. (S13)], our result does not depend on the slight difference in the parameters used in the analysis [8,58]. As x_D increases, the fraction of desorbing molecules to which a deuteron is donated through the hydrogen bond from neighboring water molecules increases, resulting in the observed x_D dependence of E_d [Fig. 2(c)], i.e., $E_d^X(\text{smaller } x_\text{D}) > E_d^X(\text{larger } x_\text{D})$. Therefore, the microscopic origin of the x_D dependence of E_d would be essentially the same with the Ubbelohde effect.

In the present study, we have demonstrated the impact of deuterium substitutions in the kinetic motion of a desorbing molecule ($E_d^{\text{H}_2\text{O}} < E_d^{\text{HDO}} < E_d^{\text{D}_2\text{O}}$) and the hydrogen-bonding interactions with neighboring molecules [$E_d^X(\text{smaller } x_\text{D}) > E_d^X(\text{larger } x_\text{D})$], on the basis of the isotope-selective measurements on the sublimation of crystalline and amorphous ices with various isotope compositions [Figs. 2(c) and S6]. The similarity of the isotope dependence was also confirmed in the evaporation of liquid water (Fig. S7). These results indicate that the observed isotopic differences in the binding energy of water aggregates are derived from the following two deuteration effects: (1) the bond-strengthening effect derived from a decrease of the zero-point energy of the hindered rotational motion of a desorbing molecule, and (2) the bond-weakening (and elongating) effect derived from the quantum anharmonic coupling between inter- and intramolecular modes relevant to hydrogen-bond breaking. These deuteration effects would also be important in partial bond-breaking processes such as structural rearrangements in bulk water systems, as will be discussed in our forthcoming paper.

Our results could also provide a reasonable interpretation on the unique isotope effects in the binding energy of water aggregates in comparison with bulky hydrogen-bonded molecules. Note that the deuteration effect (1) plays crucial roles in the bond-breaking process of extremely small and light molecules. In the case of water aggregates, the huge isotopic difference in the zero-point energy of the hindered rotation brings out the peculiar nature of the bond-strengthening effect (1) overwhelming the bond-weakening effect (2), leading to the peculiar isotope effect: Deuterated water molecules form longer but stronger hydrogen bonds than hydrogenated water molecules. In contrast, in the case of other typical hydrogen-bonded systems composed of larger and heavier constituent molecules, such as oxalic acid dihydrate, benzoic acid, succinic acid, and cyclohexane/Rh(111) [6–14], the isotopic differences in the zero-point energy of the hindered rotation are negligibly small. Therefore, only the bond-weakening effect (2) is predominant in the isotope effect on the binding energy, resulting in longer and weaker hydrogen bonds in deuterated systems than hydrogenated systems. Thus, the isotopic differences in the strength of hydrogen bonds are determined by a delicate balance between the competing deuteration effects (1) and (2), while those in the hydrogen-bond length, i.e., the geometrical isotope effect, are basically dominated by the deuteration effect (2). Our results and concepts provide a firm basis for our fundamental understanding of the isotope effects in highly quantum hydrogen-bonded systems.

We are grateful to Yuji Otsuki, Norihiro Aiga, Haruki Okuyama, Tetsuya Hama, and Shinji Saito for fruitful discussions. This work was supported by MEXT KAKENHI Grant-in-Aid for Scientific Research on Innovative Areas, No. 16H00937; JST-PRESTO JPMJPR16S7; JSPS KAKENHI Grant-in-Aid for Young Scientists (A), No. 16H06029; Grant-in-Aid for Specially Promoted Research, No. 17H06087; Grant-in-Aid for Scientific Research (A), No. 19H00865 and No. 16H02249; and Grant-in-Aid for JSPS Research Fellow, No. 17J08362.

[1] M. E. Tuckerman, D. Marx, and M. Parrinello, The nature and transport mechanism of hydrated hydroxide ions in aqueous solution, Nature (London) **417**, 925 (2002).

[2] P. A. Frey, S. A. Whitt, and J. B. Tobin, A low-barrier hydrogen bond in the catalytic triad of serine proteases, Science **264**, 1927 (1994).

[3] T. E. Markland and B. J. Berne, Unraveling quantum mechanical effects in water using isotopic fractionation, Proc. Natl. Acad. Sci. USA **109**, 7988 (2012).

[4] S. Horiuchi and Y. Tokura, Organic ferroelectrics, Nat. Mater. **7**, 357 (2008).

[5] J. Guo, J.-T. Lü, Y. Feng, J. Chen, J. Peng, Z. Lin, X. Meng, Z. Wang, X.-Z. Li, E.-G. Wang, and Y. Jiang, Nuclear quantum effects of hydrogen bonds probed by tip-enhanced inelastic electron tunneling, Science **352**, 321 (2016).

[6] M. Ichikawa, Correlation between two isotope effects in hydrogen-bonded crystals: Transition temperature and separation of two equilibrium sites, Chem. Phys. Lett. **79**, 583 (1981).

[7] T. Masanori, Isotope effect and cluster size dependence for water and hydrated hydrogen halide clusters: Multicomponent molecular orbital approach, Mol. Phys. **100**, 881 (2002).

[8] Y. Ikabata, Y. Imamura, and H. Nakai, Interpretation of intermolecular geometric isotope effect in hydrogen bonds: Nuclear orbital plus molecular orbital study, J. Phys. Chem. A **115**, 1433 (2011).

[9] K. T. Wikfeldt and A. Michaelides, Communication: *Ab initio* simulations of hydrogen-bonded ferroelectrics: Collective tunneling and the origin of geometrical isotope effects, J. Chem. Phys. **140**, 041103 (2014).

[10] R. H. McKenzie, C. Bekker, B. Athokpam, and S. G. Ramesh, Effect of quantum nuclear motion on hydrogen bonding, J. Chem. Phys. **140**, 174508 (2014).

[11] T. Koitaya and J. Yoshinobu, The quantum nature of C-H···metal interaction: Vibrational spectra and kinetic and geometric isotope effects of adsorbed cyclohexane, Chem. Rec. **14**, 848 (2014).

[12] T. Koitaya, S. Shimizu, K. Mukai, S. Yoshimoto, and J. Yoshinobu, Kinetic and geometric isotope effects originating from different adsorption potential energy surfaces: Cyclohexane on Rh(111), J. Chem. Phys. **136**, 214705 (2012).

[13] J. M. Robertson and A. R. Ubbelohde, Structure and thermal properties associated with some hydrogen bonds in crystals I. The isotope effect, Proc. R. Soc. London, Ser. A **170**, 222 (1939).

[14] S. Koval, J. Kohanoff, R. L. Migoni, and E. Tosatti, Ferroelectricity and Isotope Effects in Hydrogen-Bonded KDP Crystals, Phys. Rev. Lett. **89**, 187602 (2002).

[15] B. Stadtmüller, D. Lüftner, M. Willenbockel, E. M. Reinisch, T. Sueyoshi, G. Koller, S. Soubatch, M. G. Ramsey, P. Puschnig, F. S. Tautz, and C. Kumpf, Unexpected interplay of bonding height and energy level alignment at heteromolecular hybrid interfaces, Nat. Commun. **5**, 3685 (2014).

[16] A. M. Dolgonosov, The universal relationship between the energy and length of a covalent bond derived from the theory of generalized charges, Russ. J. Inorg. Chem. **62**, 344 (2017).

[17] Y. Harada, T. Tokushima, Y. Horikawa, O. Takahashi, H. Niwa, M. Kobayashi, M. Oshima, Y. Senba, H. Ohashi, K. T. Wikfeldt, A. Nilsson, L. G. M. Pettersson, and S. Shin, Selective Probing of the OH or OD Stretch Vibration in Liquid Water using Resonant Inelastic Soft-X-Ray Scattering, Phys. Rev. Lett. **111**, 193001 (2013).

[18] J. P. Devlin, Preferential deuterium bonding at the ice surface: A probe of surface water molecule mobility, J. Chem. Phys. **112**, 5527 (2000).

[19] J. Liu, R. S. Andino, C. M. Miller, X. Chen, D. M. Wilkins, M. Ceriotti, and D. E. Manolopoulos, A surface-specific isotope effect in mixtures of light and heavy water, J. Phys. Chem. C **117**, 2944 (2013).

[20] F. Bruni, G. Consolini, and G. Careri, Temperature dependence of dielectric relaxation in H_2O and D_2O ice: A dissipative quantum tunneling approach, J. Chem. Phys. **99**, 538 (1993).

[21] Y. Nagata, R. E. Pool, E. H. G. Backus, and M. Bonn, Nuclear Quantum Effects Affect Bond Orientation of Water at the Water-Vapor Interface, Phys. Rev. Lett. **109**, 226101 (2012).

[22] K. Röttger, A. Endriss, J. Ihringer, S. Doyle, and W. F. Kuhs, Lattice constants and thermal expansion of H_2O and D_2O ice Ih, Acta Crystallogr., Sect. B **50**, 644 (1994).

[23] B. Pamuk, J. M. Soler, R. Ramírez, C. P. Herrero, P. W. Stephens, P. B. Allen, and M.-V. Fernández-Serra, Anomalous Nuclear Quantum Effects in Ice, Phys. Rev. Lett. **108**, 193003 (2012).

[24] J. A. Smith, F. E. Livingston, and S. M. George, Isothermal desorption kinetics of crystalline H_2O, $H_2{}^{18}O$, and D_2O ice multilayers, J. Phys. Chem. B **107**, 3871 (2003).

[25] R. S. Smith, J. Matthiesen, J. Knox, and B. D. Kay, Crystallization kinetics and excess free energy of H_2O and D_2O nanoscale films of amorphous solid water, J. Phys. Chem. A **115**, 5908 (2010).

[26] W. A. Van Hook, Vapor pressures of the isotopic waters and ices, J. Phys. Chem. **72**, 1234 (1968).

[27] M. Ceriotti, W. Fang, P. G. Kusalik, R. H. McKenzie, A. Michaelides, M. A. Morales, and T. E. Markland, Nuclear quantum effects in water and aqueous systems: Experiment, theory, and current challenges, Chem. Rev. **116**, 7529 (2016).

[28] S. Habershon, T. E. Markland, and D. E. Manolopoulos, Competing quantum effects in the dynamics of a flexible water model, J. Chem. Phys. **131**, 024501 (2009).

[29] X.-Z. Li, B. Walker, and A. Michaelides, Quantum nature of the hydrogen bond, Proc. Natl. Acad. Sci. USA **108**, 6369 (2011).

[30] D. M. Wilkins, D. E. Manolopoulos, S. Pipolo, D. Laage, and J. T. Hynes, Nuclear quantum effects in water reorientation and hydrogen-bond dynamics, J. Phys. Chem. Lett. **8**, 2602 (2017).

[31] F. Paesani, S. Yoo, H. J. Bakker, and S. S. Xantheas, Nuclear quantum effects in the reorientation of water, J. Phys. Chem. Lett. **1**, 2316 (2010).

[32] K. H. Kim, H. Pathak, A. Späh, F. Perakis, D. Mariedahl, J. A. Sellberg, T. Katayama, Y. Harada, H. Ogasawara, L. G. M. Pettersson, and A. Nilsson, Temperature-Independent Nuclear Quantum Effects on the Structure of Water, Phys. Rev. Lett. **119**, 075502 (2017).

[33] J. A. Morrone and R. Car, Nuclear Quantum Effects in Water, Phys. Rev. Lett. **101**, 017801 (2008).

[34] D. E. Brown, S. M. George, C. Huang, E. K. L. Wong, K. B. Rider, R. S. Smith, and B. D. Kay, H_2O condensation coefficient and refractive index for vapor-deposited ice from molecular beam and optical interference measurements, J. Phys. Chem. **100**, 4988 (1996).

[35] T. Sugimoto, N. Aiga, Y. Otsuki, K. Watanabe, and Y. Matsumoto, Emergent high-T_c ferroelectric ordering of strongly correlated and frustrated protons in a heteroepitaxial ice film, Nat. Phys. **12**, 1063 (2016).

[36] Y. Otsuki, T. Sugimoto, T. Ishiyama, A. Morita, K. Watanabe, and Y. Matsumoto, Unveiling subsurface hydrogen-bond structure of hexagonal water ice, Phys. Rev. B **96**, 115405 (2017).

[37] N. Aiga, T. Sugimoto, Y. Otsuki, K. Watanabe, and Y. Matsumoto, Origins of emergent high-T_c ferroelectric ordering in heteroepitaxial ice films: Sum-frequency generation vibrational spectroscopy of H_2O and D_2O ice films on Pt(111), Phys. Rev. B **97**, 075410 (2018).

[38] K. Thürmer and S. Nie, Formation of hexagonal and cubic ice during low-temperature growth, Proc. Natl. Acad. Sci. USA **110**, 11757 (2013).

[39] A. Glebov, A. P. Graham, A. Menzel, J. P. Toennies, and P. Senet, A helium atom scattering study of the structure and phonon dynamics of the ice surface, J. Chem. Phys. **112**, 11011 (2000).

[40] G. Zimbitas and A. Hodgson, The morphology of thin water films on Pt(111) probed by chloroform adsorption, Chem. Phys. Lett. **417**, 1 (2006).

[41] G. A. Kimmel, N. G. Petrik, Z. Dohnálek, and B. D. Kay, Crystalline ice growth on Pt(111) and Pd(111): Nonwetting growth on a hydrophobic water monolayer, J. Chem. Phys. **126**, 114702 (2007).

[42] G. A. Kimmel, N. G. Petrik, Z. Dohnálek, and B. D. Kay, Crystalline Ice Growth on Pt(111): Observation of a Hydrophobic Water Monolayer, Phys. Rev. Lett. **95**, 166102 (2005).

[43] J. Meija, Z. Mester, and A. D'Ulivo, Mass spectrometric separation and quantitation of overlapping isotopologues. $H_2O/HOD/D_2O$ and $H_2Se/HDSe/D_2Se$ mixtures, J. Am. Soc. Mass Spectrom. **17**, 1028 (2006).

[44] A. A. Christy, F. O. Libnau, and O. M. Kvalheim, Determination of the equilibrium constant and resolution of the HOD spectrum by alternating least-squares and infrared analysis, Appl. Spectrosc. **49**, 1431 (1995).

[45] S. Kim, E. Park, and H. Kang, Segregation of hydroxide ions to an ice surface, J. Chem. Phys. **135**, 074703 (2011).

[46] R. S. Smith, C. Huang, and B. D. Kay, Evidence for molecular translational diffusion during the crystallization of amorphous solid water, J. Phys. Chem. B **101**, 6123 (1997).

[47] See Supplemental Material at http://link.aps.org/supplemental/10.1103/PhysRevMaterials.3.112001 for experimental details, supporting discussions of our TST model, LS model, deuter-

ation effects on the sublimation of amorphous ice and the evaporation of liquid water, the previously proposed desorption mechanism, the equilibrium constant K for isotope scrambling, and the ferroelectric proton ordering, which contains Refs. [60–83].

[48] P. A. Redhead, Thermal desorption of gases, Vacuum **12**, 203 (1962).

[49] W. Linert and R. F. Jameson, The isokinetic relationship, Chem. Soc. Rev. **18**, 477 (1989).

[50] A. Redondo, Y. Zeiri, J. J. Low, and W. A. Goddard, Application of transition state theory to desorption from solid surfaces: Ammonia on Ni(111), J. Chem. Phys. **79**, 6410 (1983).

[51] W. J. Smit, F. Tang, M. A. Sánchez, E. H. G. Backus, L. Xu, T. Hasegawa, M. Bonn, H. J. Bakker, and Y. Nagata, Excess Hydrogen Bond at the Ice-Vapor Interface around 200 K, Phys. Rev. Lett. **119**, 133003 (2017).

[52] T. Sugimoto, Y. Otsuki, T. Ishiyama, A. Morita, K. Watanabe, and Y. Matsumoto, Topologically disordered mesophase at the topmost surface layer of crystalline ice between 120 and 200 K, Phys. Rev. B **99**, 121402 (2019).

[53] V. Buch and J. P. Devlin, Spectra of dangling OH bonds in amorphous ice: Assignment to 2- and 3-coordinated surface molecules, J. Chem. Phys. **94**, 4091 (1991).

[54] V. F. Petrenko and R. W. Whitworth, *Physics of Ice* (Oxford University Press, New York, 1999).

[55] E. R. Lippincott and R. Schroeder, One-dimensional model of the hydrogen bond, J. Chem. Phys. **23**, 1099 (1955).

[56] A. M. Dokter and H. J. Bakker, Transient absorption of vibrationally excited ice Ih, J. Chem. Phys. **128**, 024502 (2008).

[57] F. Perakis, S. Widmer, and P. Hamm, Two-dimensional infrared spectroscopy of isotope-diluted ice Ih, J. Chem. Phys. **134**, 204505 (2011).

[58] K. Ando, Semiquantal analysis of hydrogen bond, J. Chem. Phys. **125**, 014104 (2006).

[59] T. Saitoh, K. Mori, and R. Itoh, Two-dimensional vibrational analysis of the Lippincott-Schröder potential for OH-O, NH-O, and NH-N hydrogen bonds and the deuterium isotope effect, Chem. Phys. **60**, 161 (1981).

[60] S. Haq, J. Harnett, and A. Hodgson, Growth of thin crystalline ice films on Pt(111), Surf. Sci. **505**, 171 (2002).

[61] T. Sugimoto and K. Fukutani, Effects of Rotational-Symmetry Breaking on Physisorption of Ortho- and Para-H_2 on Ag(111), Phys. Rev. Lett. **112**, 146101 (2014).

[62] J. L. Daschbach, B. M. Peden, R. S. Smith, and B. D. Kay, Adsorption, desorption, and clustering of H_2O on Pt(111), J. Chem. Phys. **120**, 1516 (2004).

[63] X. Su, L. Lianos, Y. R. Shen, and G. A. Somorjai, Surface-Induced Ferroelectric Ice on Pt(111), Phys. Rev. Lett. **80**, 1533 (1998).

[64] Y. Lilach, M. J. Iedema, and J. P. Cowin, Dissociation of Water Buried under Ice on Pt(111), Phys. Rev. Lett. **98**, 016105 (2007).

[65] Y. Lilach, M. J. Iedema, and J. P. Cowin, Proton segregation on a growing ice interface, Surf. Sci. **602**, 2886 (2008).

[66] G. Zimbitas, M. E. Gallagher, G. R. Darling, and A. Hodgson, Wetting of mixed OH/H_2O layers on Pt(111), J. Chem. Phys. **128**, 074701 (2008).

[67] I. Waluyo, D. Nordlund, L.-Å. Näslund, H. Ogasawara, L. G. M. Pettersson, and A. Nilsson, Spectroscopic evidence for the formation of 3-D crystallites during isothermal heating of amorphous ice on Pt(111), Surf. Sci. **602**, 2004 (2008).

[68] J. Harnett, S. Haq, and A. Hodgson, Electron induced restructuring of crystalline ice adsorbed on Pt(111), Surf. Sci. **528**, 15 (2003).

[69] S. Meng, E. G. Wang, and S. Gao, Water adsorption on metal surfaces: A general picture from density functional theory studies, Phys. Rev. B **69**, 195404 (2004).

[70] S. Nie, P. J. Feibelman, N. C. Bartelt, and K. Thürmer, Pentagons and Heptagons in the First Water Layer on Pt(111), Phys. Rev. Lett. **105**, 026102 (2010).

[71] S. Standop, A. Redinger, M. Morgenstern, T. Michely, and C. Busse, Molecular structure of the H_2O wetting layer on Pt(111), Phys. Rev. B **82**, 161412 (2010).

[72] S. Maier, B. A. J. Lechner, G. A. Somorjai, and M. Salmeron, Growth and structure of the first layers of ice on Ru(0001) and Pt(111), J. Am. Chem. Soc. **138**, 3145 (2016).

[73] W. S. Benedict, N. Gailar, and E. K. Plyler, Rotation-vibration spectra of deuterated water vapor, J. Chem. Phys. **24**, 1139 (1956).

[74] Y. Nagata, K. Usui, and M. Bonn, Molecular Mechanism of Water Evaporation, Phys. Rev. Lett. **115**, 236102 (2015).

[75] K. Ohno, M. Okimura, N. Akai, Y. Katsumoto, K. Aoki, and T. A. Beu, The effect of cooperative hydrogen bonding on the OH stretching-band shift for water clusters studied by matrix-isolation infrared spectroscopy and density functional theory, Phys. Chem. Chem. Phys. **7**, 3005 (2005).

[76] C. J. Tainter and J. L. Skinner, The water hexamer: Three-body interactions, structures, energetics, and OH-stretch spectroscopy at finite temperature, J. Chem. Phys. **137**, 104304 (2012).

[77] A. Wong, L. Shi, R. Auchettl, D. McNaughton, D. R. T. Appadoo, E. G. Robertson, S. Bauerecker, J. Zhou, and C. M. Wright, Heavy snow: IR spectroscopy of isotope mixed crystalline water ice, Phys. Chem. Chem. Phys. **18**, 4978 (2016).

[78] M. V. Vener, How reliable is the Lippincott-Schroeder potential for the OH$\cdots$N hydrogen bonded fragment in the gas phase? Chem. Phys. Lett. **244**, 89 (1995).

[79] C. D. Cappa, W. S. Drisdell, J. D. Smith, R. J. Saykally, and R. C. Cohen, Isotope fractionation of water during evaporation without condensation, J. Phys. Chem. B **109**, 24391 (2005).

[80] C. D. Cappa, J. D. Smith, W. S. Drisdell, R. J. Saykally, and R. C. Cohen, Interpreting the H/D isotope fractionation of liquid water during evaporation without condensation, J. Phys. Chem. C **111**, 7011 (2007).

[81] D. M. Murphy and T. Koop, Review of the vapour pressures of ice and supercooled water for atmospheric applications, Q. J. R. Meteorol. Soc. **131**, 1539 (2005).

[82] T. J. Chuang, H. Seki, and I. Hussla, Infrared photodesorption: Vibrational excitation and energy transfer processes on surfaces, Surf. Sci. **158**, 525 (1985).

[83] P. A. Thiel, The interaction of water with solid surfaces: Fundamental aspects, Surf. Sci. Rep. **7**, 211 (1987).